

Yavuz Hakan Ozdemir
Baris Barlas
Tamer Yilmaz
Seyfettin Bayraktar

ISSN 0007-215X
eISSN 1845-5859

NUMERICAL AND EXPERIMENTAL STUDY OF TURBULENT FREE SURFACE FLOW FOR A FAST SHIP MODEL

UDC 629.5.015.2
Original scientific paper

Summary

In this study the experimental and computational results for a fast ship model is presented. The Reynolds Averaged Navier Stokes (RANS) equations and the nonlinear free surface boundary conditions are discretized by means of an overset grid finite volume scheme. The experiments are performed at Istanbul Technical University Towing Tank basin. In the numerical turbulent flow calculations, the relationship between the Boussinesq's hypothesis of turbulence viscosity and the velocities are obtained through the standard $k-\varepsilon$ turbulence model. Simulations of turbulent free surface flows around the model are performed by using Star CCM+ solver and Volume of Fluid (VOF) model to capture the free surface between air and water. The total resistance of the ship model is compared with the experimental results. Bow and aft wave form developments are also investigated qualitatively. For Froude (Fn) numbers less than 0.25, the computations are found to be well satisfactory, giving efficient and accurate tool to predict curves of resistance. For relatively higher speeds ($Fn > 0.25$) a low Reynolds number turbulence model may be more suitable to predict the resistance.

Key words: *CFD, Turbulent free surface flows, Star CCM+, fast hull, $k-\varepsilon$ turbulence model.*

1. Introduction

Investigation of flow around a hull has been done for years. Most of initial works had been done experimentally due to lack of advanced numerical techniques and insufficient computational resources. Recently advances of computing technology have enabled the researchers to conduct their researches numerically. By means of the presence of advanced numerical techniques, software and hardware almost all kinds of problems that can occur in real situations can be simulated nowadays and validated with experimental data in confidence.

In spite of its current fame, results obtained by computational fluid dynamics (CFD) techniques were very poor and consisted very little information about the flow. CFD based

approaches assumed the flow as inviscid since the solution of Navier-Stokes equation was difficult to solve in the past. As aforementioned, the recent progress of computing technology enables researchers to solve the problems by means of Reynolds-Averaged Navier-Stokes (RANS), Large Eddy Simulation (LES) and Direct Numerical Solution (DNS). Main drawback of LES and DNS is that they require more memory and fast computers. Therefore, RANS based solutions have been used widely in shipbuilding industry.

It can be reviewed from the literature that ship hydrodynamics computations based on RANS solvers were initiated in the 1980s, and since then a number of useful codes have been developed [1]. In recent years, computational fluid dynamics (CFD) techniques have been incorporated into optimization procedures for hull configuration. Thus, CFD simulations play an important role in ship design, performance analysis and form optimization. Gorski, Bulgarelli et al., Parolini and Quarteroni, Ahmed et al., and Sridhar et al. reported innovative aspects of the numerical models used in CFD studies [2-6]. Flow around a ship hull is a free surface flow that a liquid comes in contact with a gas. The liquid-gas interface shows highly severe surface force and causes a complex flow. Due to its complexity several experimental and numerical studies have been performed by several researchers, reviews can be found in Wackers et al. [7], and Xing et al. [8]. Tinquiu et al. describes a method for simulation of viscous flows around realistic hull forms with a moving mesh [9]. Leroyer et al. presents two numerical procedures to speed up computations when dealing with a RANS solver based on the VOF method to treat the free surface [10]. Recently, Guo et al. studied the prediction of added resistance and ship motion of KVLCC2 model in head waves by using RANS equations [11]. Kandasamy et al. studied the CFD validation for high-speed passenger-only ferries aimed at reducing far-field wake energy that causes beach erosion [12]. The validation procedure used full-scale measurements of resistance, sinkage, trim, and far-field wake train obtained over a wide range of speeds for two highspeed semi-planing foil-assisted catamarans. Takai et al. worked on waterjet propulsion using CFD for performance analyses of existing waterjet designs as well as for the improvement and design optimization of new waterjet propulsion systems for high-speed marine vehicles [13]. Seo et al. investigated 3600 TEU container ship with an inclined keel and its further validation for the bare hull resistance analysis by using Star CCM+ and large scale model tests [14].

In the present study, unsteady turbulent flow around a fast ship hull is investigated numerically and experimentally. Numerical analyses are done by means of RANS solution. The model experiments were conducted at Istanbul Technical University Ata Nutku Towing Tank to validate the computational results and to evaluate the total resistance. The turbulence model used is the well-known standard $k-\varepsilon$ two equation turbulence model. The numerical algorithm is divided into three stages: in the first stage the velocity components, in the second stage the pressure and in the third stage the turbulence quantities are calculated by using the overset grid finite volume method discretization of the spatial domain. The main goal of this study is to show the capability of general purpose CFD code of Star CCM+ for design, analysis and reliability for fast ship hulls. Uncertainty analysis shows that the grid dependency of the solution in ship resistance is low. Three grid systems (coarse, medium and fine) are utilized and the solutions from a medium grid are sufficient to study the general trend of flow.

The following section provides brief explanations about the governing equations, boundary conditions. Section 3 gives the experimental procedure, while, Section 4 introduces the numerical approach. Results and discussions are presented in Section 5. Finally, the conclusion indicates that for Froude numbers less than 0.25, Star CCM+ successfully

estimates the general trend of flow around a fast ship hull, for Froude numbers higher than 0.25 a low Reynolds number turbulence model may be more suitable.

2. Mathematical formulation

2.1 Governing equations

The governing equations are continuity and momentum equations for the unsteady, three-dimensional incompressible flow. The continuity equation and momentum equations in Cartesian coordinates can be given as;

$$\frac{\partial U_i}{\partial x_i} = 0 \quad (1)$$

for the continuity,

$$\frac{\partial U_i}{\partial t} + \frac{\partial(U_i U_j)}{\partial x_j} = -\frac{1}{\rho} \frac{\partial p}{\partial x_i} + \frac{\partial}{\partial x_j} \left[\nu \left(\frac{\partial U_i}{\partial x_j} + \frac{\partial U_j}{\partial x_i} \right) \right] - \frac{\partial \overline{u'_i u'_j}}{\partial x_j} \quad (2)$$

for the momentum equations. Where U_i and u'_i express the mean and fluctuation velocity component in the direction of the Cartesian coordinate x_i , P the mean pressure, ρ the density and ν the kinematic viscosity. The Reynolds stress tensor is then calculated using the well-known Boussinesq's hypothesis;

$$\overline{u'_i u'_j} = -\nu_t \left(\frac{\partial U_i}{\partial x_j} + \frac{\partial U_j}{\partial x_i} \right) + \frac{2}{3} \delta_{ij} k \quad (3)$$

The eddy viscosity ν_t is calculated by combining turbulent kinetic energy, k , and the rate of dissipation of the turbulent energy, ε as follows,

The standard k - ε two equation turbulence model has been used to simulate the turbulent flows. The turbulent kinetic energy, k , and the rate of dissipation of the turbulent energy, ε , are:

$$\frac{\partial k}{\partial t} + \frac{\partial(k U_j)}{\partial x_j} = \frac{\partial}{\partial x_j} \left[\left(\nu + \frac{\nu_t}{\sigma_k} \right) \frac{\partial k}{\partial x_j} \right] + P_k - \varepsilon \quad (4)$$

$$\frac{\partial \varepsilon}{\partial t} + \frac{\partial(\varepsilon U_j)}{\partial x_j} = \frac{\partial}{\partial x_j} \left[\left(\nu + \frac{\nu_t}{\sigma_\varepsilon} \right) \frac{\partial \varepsilon}{\partial x_j} \right] + C_{\varepsilon 1} P_k \frac{\varepsilon}{k} - C_{\varepsilon 2} \frac{\varepsilon^2}{k} \quad (5)$$

where, production of kinetic energy $P_k = -\overline{u'_i u'_j} \frac{\partial U_i}{\partial x_j}$, $C_{\varepsilon 1}=1.44$, $C_{\varepsilon 2}=1.92$, $C_\mu=0.09$,

turbulent Prandl numbers for k and ε are $\sigma_k = 1.0$, and $\sigma_\varepsilon = 1.3$ respectively.

The use of standard k - ε two equation turbulence model formulation is reasonably robust and reliable near solid boundaries and recirculation regions like ship boundary layers. The pressure field is solved by using the well-known SIMPLE algorithm [15].

Calculations are made in structured overset grid computational domain for the model hull symmetric to its centerline. The general view of the computational domain with the model hull and the notations of boundary conditions are depicted in Fig. 1. The flow field is

initially taken as two ship-lengths at the front of the ship, three ship-lengths behind the ship and two ship-lengths along the beam and depth directions, respectively.

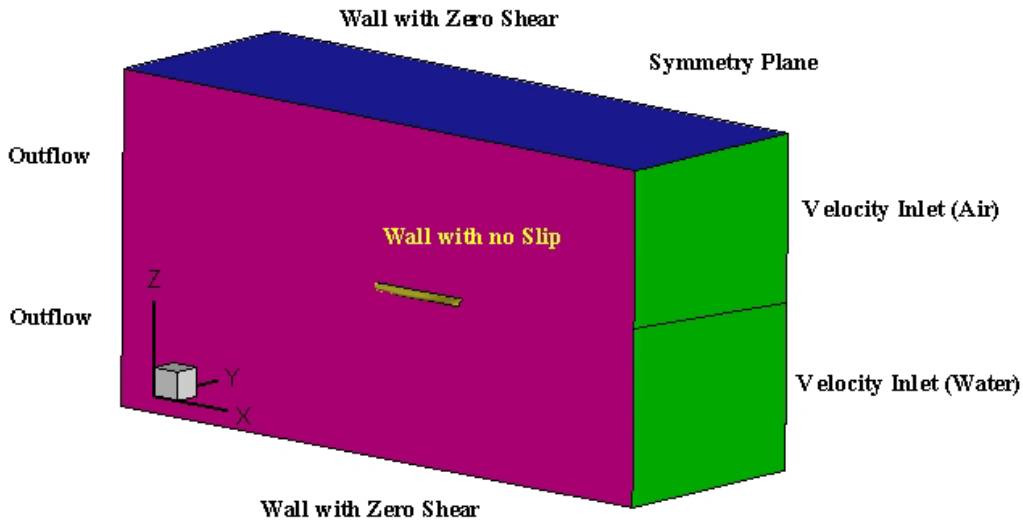


Fig. 1 The general view of the domain and boundary conditions

2.2 Boundary conditions

At inlet, U is ranging from 0.634 - 1.758 m/s. At far field, wall with slip, i.e., all the normal velocities normal to free slip wall is zero. At ship hull, wall with no slip condition, and the gradient of velocity parallel to wall is zero, as the wall shear stress is zero under free slip condition. On the first grid point of the body, k and ε become;

$$k = \frac{U_{\tau}^2}{\sqrt{\beta^*}}, \quad \varepsilon = \beta^{*3/4} \frac{k^{3/2}}{\kappa y} \quad (6)$$

Towards the outer part of the viscous sub layer and the buffer layer, the turbulence is rapidly increased by the production of turbulent kinetic energy. With the use of standard k - ε two equation turbulence model, additional wall functions are necessary to bridge the solution variables in the viscosity affected region. The velocity in the log-law region varies logarithmically with y^+ as given by Eq. (8). Although there is a slight variation in the values of universal constants in the literature [16], according to Stanford conventions suggest the von Karman constant κ as 0.41 and the equation constant B as 5.0.

$$U^+ = \frac{1}{\kappa} \ln(y^+) + B \quad (7)$$

where U^+ is the stream wise velocity non-dimensionalized by the friction velocity, u_{τ} , y^+ is the normalized wall distance such that $y^+ = yu_{\tau}/\nu$. At the upstream boundary, the uniform flow condition is used. At the downstream boundary, zero derivative condition in x -direction is used, and pressure P is taken as hydrostatic. At the symmetry plane boundaries zero derivative condition in the normal directions are utilized.

3. Experimental work

This study investigates a fast ship hull advancing in water with a free surface at different speeds. Fn used in this work is model scale. The fast ship hull is developed by Sener [17]. Experiments were carried out at the Ata Nutku Ship Model Testing Laboratory of Istanbul Technical University. The resistance measurements were performed in the Large Towing Tank of the Ata Nutku Ship Model Testing Laboratory, which is 160 m long, 6 m wide and has a water depth of 3.4 m. Detailed elevation view of the towing tank is given in Fig. 2. In the resistance tests, the hull model was fitted to the carriage and tests were carried out using an Atwood type dynamometer. The carriage speed was controlled digitally and recorded on a computer. The maximum carriage speed of the towing tank is 5.5 m/s.

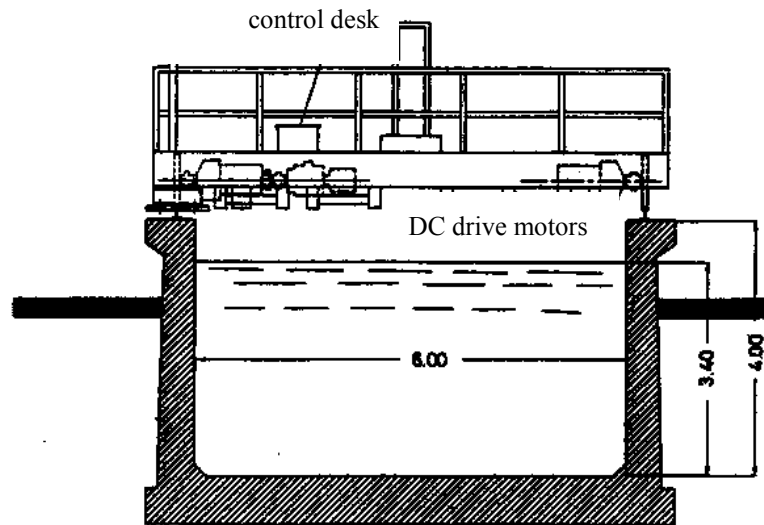


Fig. 2 Schematic view of Istanbul Technical University Ata Nutku Towing Tank

Table 1 Model ship particulars

	<i>Ship Prototype</i>	<i>Model M367</i>
Lenght on the waterline L_{WL}	139.07	3.863
Lenght between perpendiculars L_{BP}	139	3.861
Moulded breadth B	18.20	0.506
Moulded depth to upper deck D	11.20	0.31
Design draft T	5.05	0.140
Block coefficient C_B	0.489	0.489
Midship coefficient C_M	0.810	0.810
Prismatic coefficient C_P	0.605	0.605
Waterline coefficient C_{WP}	0.793	0.793
Design speed V_S	18 kts	2.572 m/s
Displacement volume ∇	5768.24	0.124
Wetted surface area A_{WS}	2550.30	1.968
Total rudder area A_R	56.66	0.043

The model is constructed on 1/36 scale with the model number M367. The ship model was made of wood. The hull geometry is depicted in Fig. 3. Waterline and profile view is given in Fig. 4. Fig. 5 shows the constructed model of the M367. In the resistance analysis, the effect of the wind was not taken into account. Turbulence stimulation was obtained by the application of studs behind the bow as well as on the rudder. The ship model was tested in calm water free to surge, heave and trim sinkage and fixed to roll, sway and yaw motions. Table 1 gives the model ship and main ship particulars. Towing tank test conditions are given in Table 2. It must be noted that the errors related to the measured data is not within the scope of this work.

Table 2 Towing tank test conditions

<i>Test conditions</i>	
Temperature ($^{\circ}\text{C}$)	16
Density ($\frac{\text{kg}}{\text{m}^3}$)	998.9
Gravitational acceleration ($\frac{\text{m}}{\text{s}^2}$)	9.802686
Kinematic viscosity (cSt)	1.10966

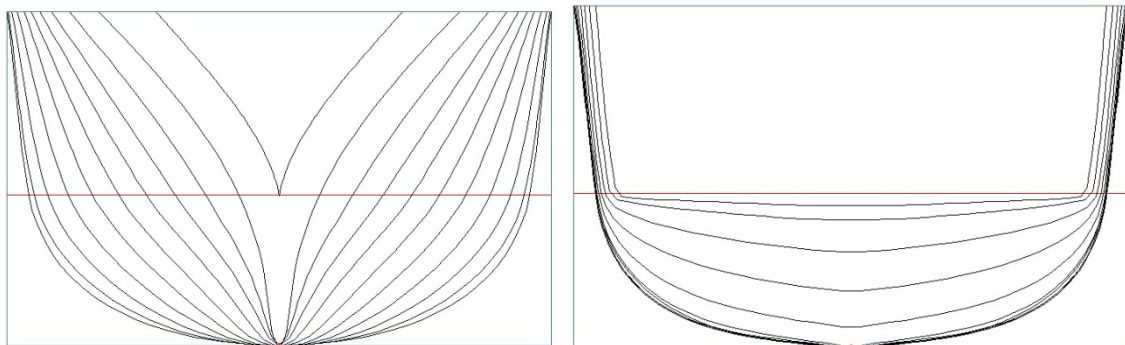


Fig. 3 Hull line of M367 ship model

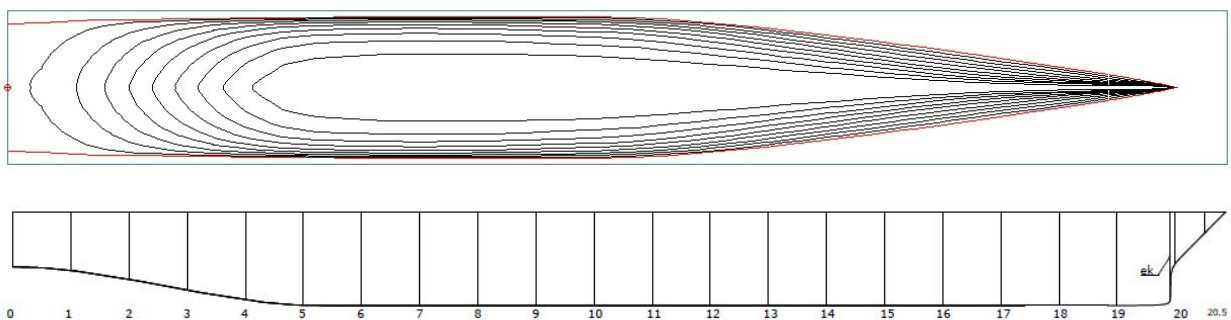


Fig. 4 Waterline and profile view of M367 ship model



Fig. 5 Views of the M367 ship model

4. Numerical approach

In this study the flow around the model ship hull was simulated by RANS based code STAR-CCM+ which enables three dimensional, VOF model simulations to capture the free surface between air and water [10,14]. The standard $k-\varepsilon$ two equation turbulence model, with near-wall function to describe the velocity profile near the wall, was used. For ship hull forms, generating good structured grids is not only an important factor in getting reliable numerical solutions, but also very difficult because of the geometric complexity of the ship's bow and aft forms. Computational grids at the ship's bow and aft are depicted in Fig. 6. The CAD design of the M367 model is given in Fig. 7. Finite volume mesh was generated entirely with overset structured cells as shown in Fig. 8 for the M367 model. The computational domain extends from $-3.0 L_{BP} < x < 3.0 L_{BP}$, $0.0 < y < 2.0 L_{BP}$ and $-1.0 L_{BP} < z < 1.0 L_{BP}$, where half of the entire computational domain was taken into account due to vertical plane symmetry. The ship axis is located along the x-axis with the bow located at $x = L_{BP}$ and the stern at $x = 0$. The still water level lies at $z = 0$.

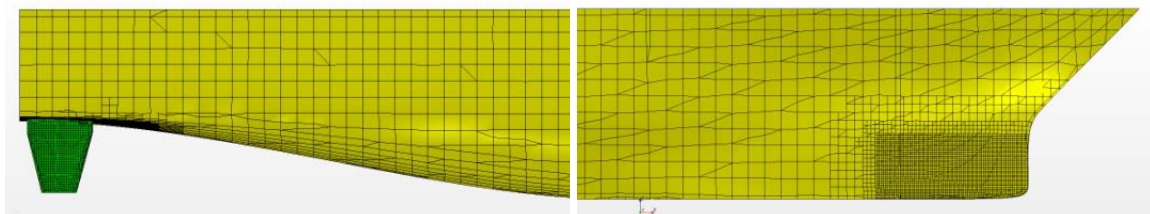


Fig. 6 Computational grids at the ship's forehead and aft end

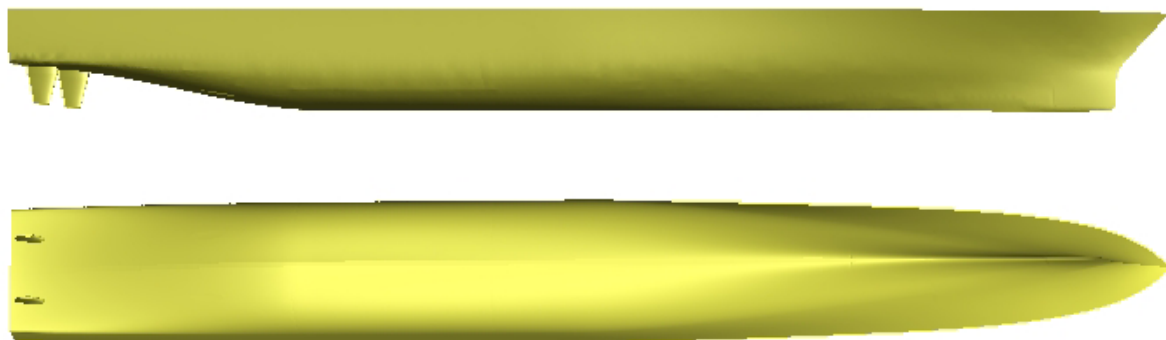


Fig. 7 The CAD design of the M367 model

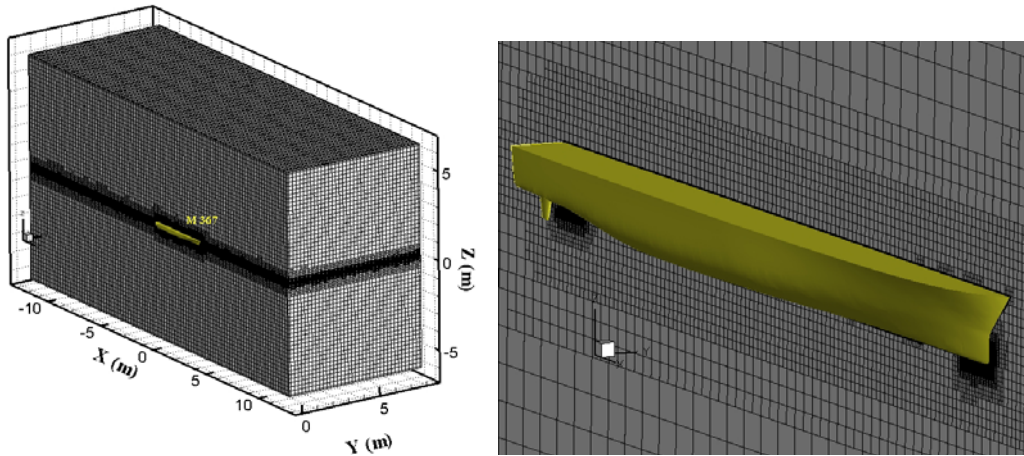


Fig. 8 The numerical grids for the M367 model

Since CFD results might contain some numerical errors, i.e. truncation errors, inappropriate initial and boundary conditions, grid dependent solutions, weak turbulence model, etc., it is important to compare the computed result with experimental data to determine the difference between the computations and the experiment. However, both computation and experiment may contain errors which in some cases result in a misrepresentative picture of the CFD code consistency. It is therefore necessary to do a grid refinement study in order to estimate the grid related uncertainty. In this work, numerical errors due to the grids were aimed to reduce by using finer grids. For numerical solution of the governing equations the domain was discretized in three different resolutions as coarse (649,300), medium (1,344,206) and fine (3,462,161). The numerical grid system employed for the verification study are shown in Fig. 9 and the total grid points for the three grid systems are given in Table 3.

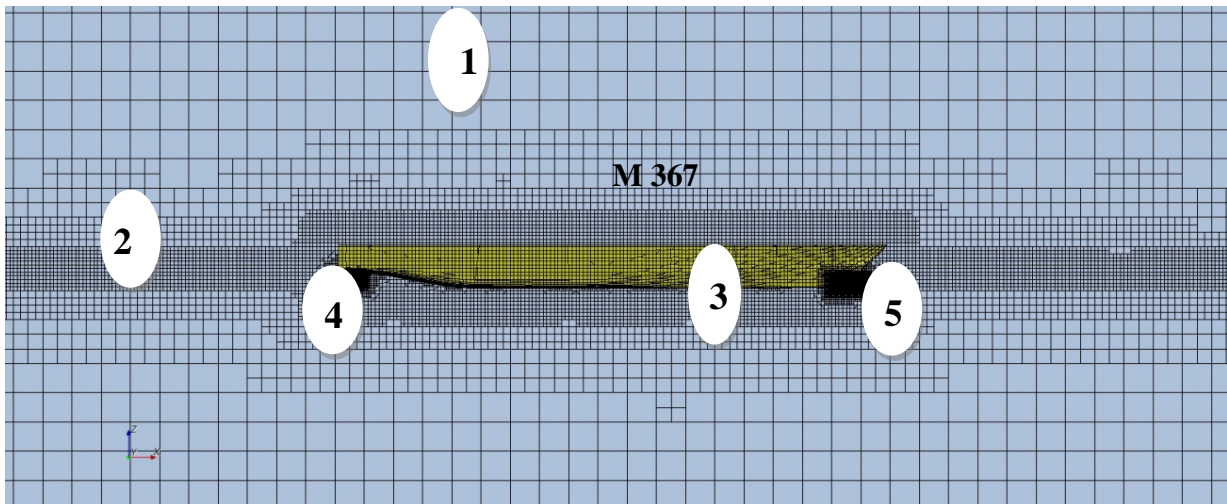


Fig. 9 The numerical grids for the M367 model, close-up view

Table 3 Grid analysis

<i>Block #</i>	<i>Block Name</i>	<i>Coarse grids</i>	<i>Medium grids</i>	<i>Fine grids</i>
1	Control volume	0.12 L	0.085 L	0.06 L
2	Free surface	0.014 L	0.01 L	0.007 L
3	Near ship	0.014 L	0.01 L	0.007 L
4	Ship's aft-end	0.0028 L	0.002 L	0.0014 L
5	Ship's fore-head	0.0028 L	0.002 L	0.0014 L

The number of grid points and average y^+ values are given in Table 4, and all the y^+ values for the medium grids can be seen on Fig. 10. The experimental and computed drag and required time for $Fn=0.201$ for three different resolutions is compared in Table 5. For coarse grid and $Fn=0.201$, the difference between computation and the experimental result is 11.42%. For medium and fine grids the difference between computation and the experimental results are less than 1% but the required time for reaching the converged solution for this case is 53 hours longer in fine grid. It is concluded that using medium grids are good enough to predict the resistance and all simulations were performed with medium grids.

Table 4 The number of grid points and average y^+ values (of the first grid point)

	<i>Coarse grids</i>	<i>Medium grids</i>	<i>Fine grids</i>
Number of Nodes	649,300	1,344,206	3,462,161
Average y^+	110	66	49

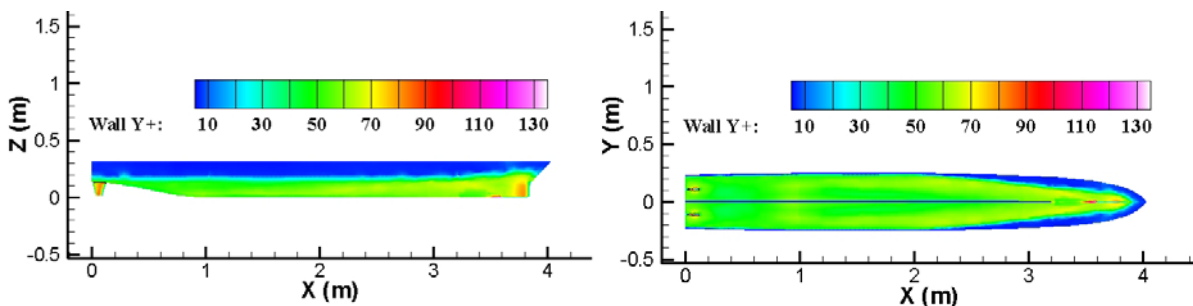


Fig. 10 The experimental and computed total resistance for the M367 model

Table 5 Experimental and computed drag required time for different grid resolutions for $Fn=0.201$

	<i>Experiment</i>	<i>Coarse grid</i>	<i>Medium grid</i>	<i>Fine grid</i>
Total Resistance (R_T) [N]	6.874	7.659	6.892	6.837
Required time [hour]	754	31	48	101

The governing equations described above are discretized using a node based finite volume method, the advection terms are discretized using a first-order upwind interpolation scheme. The governing equations are solved successively. The Courant-Frederich-Lewis (CFL) number in the main flow direction, i.e. $U\Delta t/\Delta x$ should be less than unity for better results. In the present computations the CFL number for each node on the M367 ship model is in the range between 0.3 and 0.6. The structured overset finite volume discretization of the spatial domain (Fig. 2) is performed with Star CCM+ and CAD geometry with GAMBIT preprocessor package. Since the computations involve certain approximations, an iterative procedure is needed. The solution is considered converged when the normalized residual of

free surface elevation is less than 10^{-2} in the VOF module, and residuals of all the remaining variables are less than 10^{-5} . The computations are made on an 8 CPU workstation with 3.4GHz, on windows Win7 system.

5. Results and discussions

The experiments were carried out in 11 different speeds. $(1+k)$ is the form factor determined from the resistance tests. As the form factor approach assumes that the viscous resistance is proportional to the frictional resistance coefficient of a flat plate at equal Reynolds number, the form factor is determined from simultaneous measurements of low speed total resistance. But accurate measurement of very low speed total resistance is questionable. Therefore the resistance tests started from $Fn=0.103$, which is considered as a low enough speed and the result can be plausible [18]. The total resistance coefficient of a model ship is given by

$$C_{TM} = (1+k)C_{FM} + C_W \quad (8)$$

where C_{FM} is the frictional resistance coefficient, C_W is the wave making resistance coefficient of the model ship. First, sets of Froude numbers versus C_{TM}/C_{FM} values are computed. These data sets are curve fitted by using linear regression approach.

$$\frac{C_{TM}}{C_{FM}} = aFn + b \quad (9)$$

By definition, the form factor can be expressed as

$$1+k = \lim_{Fn \rightarrow 0} \frac{C_{TM}}{C_{FM}} \quad (10)$$

The form factor thus becomes the constant term, b . The form factor was calculated using Prohaska's method [19] both from the experiments and the computations as 1.241 and 1.205 respectively as shown in Table 6. The RANS computations predict a 2.92% lower form factor compared to the model test results.

Table 6 Form factor prediction from experiment and computed results

	$1+k$	Difference
Experiment	1.241	
Computation	1.205	-2.92%

Table 7 shows the measured total resistance and total resistance coefficient, the computed total resistance and total resistance coefficient, and the difference between computation and the experiment for given speeds. The model experiments at low speeds can be questionable, but according to the uncertainty analysis [20] the error should be in the range of $\pm 1.5\%$. The comparison with the experimental measures is very good for $0.103 \leq Fn \leq 0.239$. Within the given range, the maximum error is 5.90% (± 1.5) at $Fn=0.239$. The RANS computations generally predicted lower total resistance values. The model tests indicate that the computations predicted 9.44% lower total resistance at $Fn=0.264$, 12.40% lower total resistance at $Fn=0.286$ and 17.96% lower total resistance at $Fn=0.322$. In this work the standard $k-\varepsilon$ two equation turbulence model with near-wall function was used.

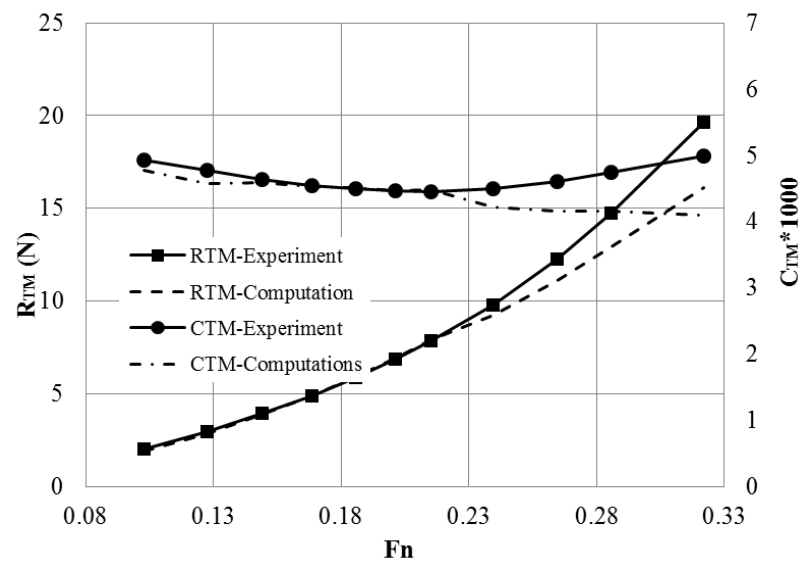


Fig. 11 Computed and measured total resistance and total resistance coefficient for M367 model

Table 7 Resistance results

F_n	V [m/s]	<i>Experiment</i>		<i>CFD</i>		<i>Difference</i>
		R_{TM} [N]	C_{TM} (x1000)	R_{TM} [N]	C_{TM} (x1000)	
0.103	0.634	1.988	4.928	1.926	4.775	-3.11%
0.127	0.784	2.947	4.773	2.822	4.571	-4.23%
0.149	0.918	3.913	4.627	3.879	4.586	-0.88%
0.168	1.037	4.902	4.540	4.893	4.532	-0.18%
0.186	1.143	5.893	4.489	5.929	4.516	0.60%
0.201	1.239	6.874	4.461	6.892	4.472	0.26%
0.215	1.325	7.845	4.452	7.900	4.483	0.71%
0.239	1.474	9.785	4.488	9.208	4.223	-5.90%
0.264	1.628	12.245	4.597	11.090	4.163	-9.44%
0.286	1.758	14.736	4.741	12.909	4.153	-12.40%
0.322	1.980	19.650	4.982	16.123	4.087	-17.96%

With this approach it is not possible to forecast the boundary layer separation at the stern flow that increase the resistance of the ship model, therefore at higher speeds another type of turbulence model which is capable of capturing the flow separation can be used to better predict the flow characteristics. Computed and measured total resistance and total resistance coefficient for M367 model can be seen at Fig. 11.

The wave cut results of the longitudinal wave profiles at $y/L_{BP}=0.035$ for $F_n=0.168$, $F_n=0.264$ and $F_n=0.322$ are presented qualitatively in Fig. 12. Fig. 13 shows computed wave patterns of the model hull for 6 different speeds, using medium grids, where the bow and stern wave elevations can be seen clearly.

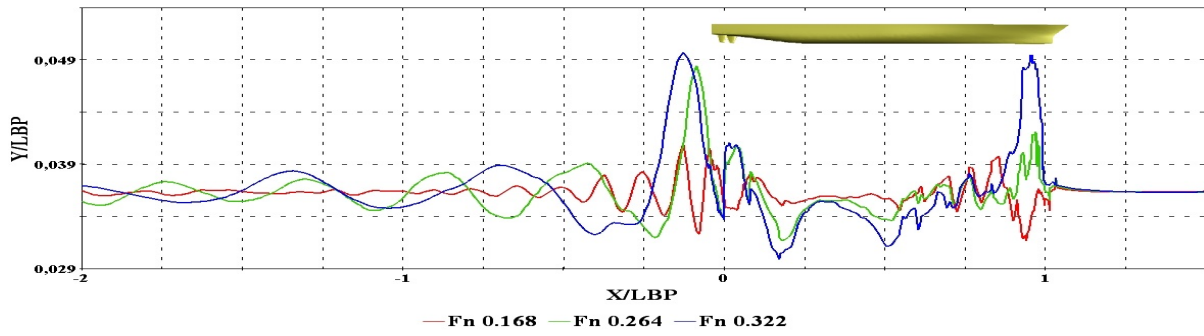


Fig. 12 Free surface deformation for $F_n=0.168$, $F_n=0.264$ and $F_n=0.322$

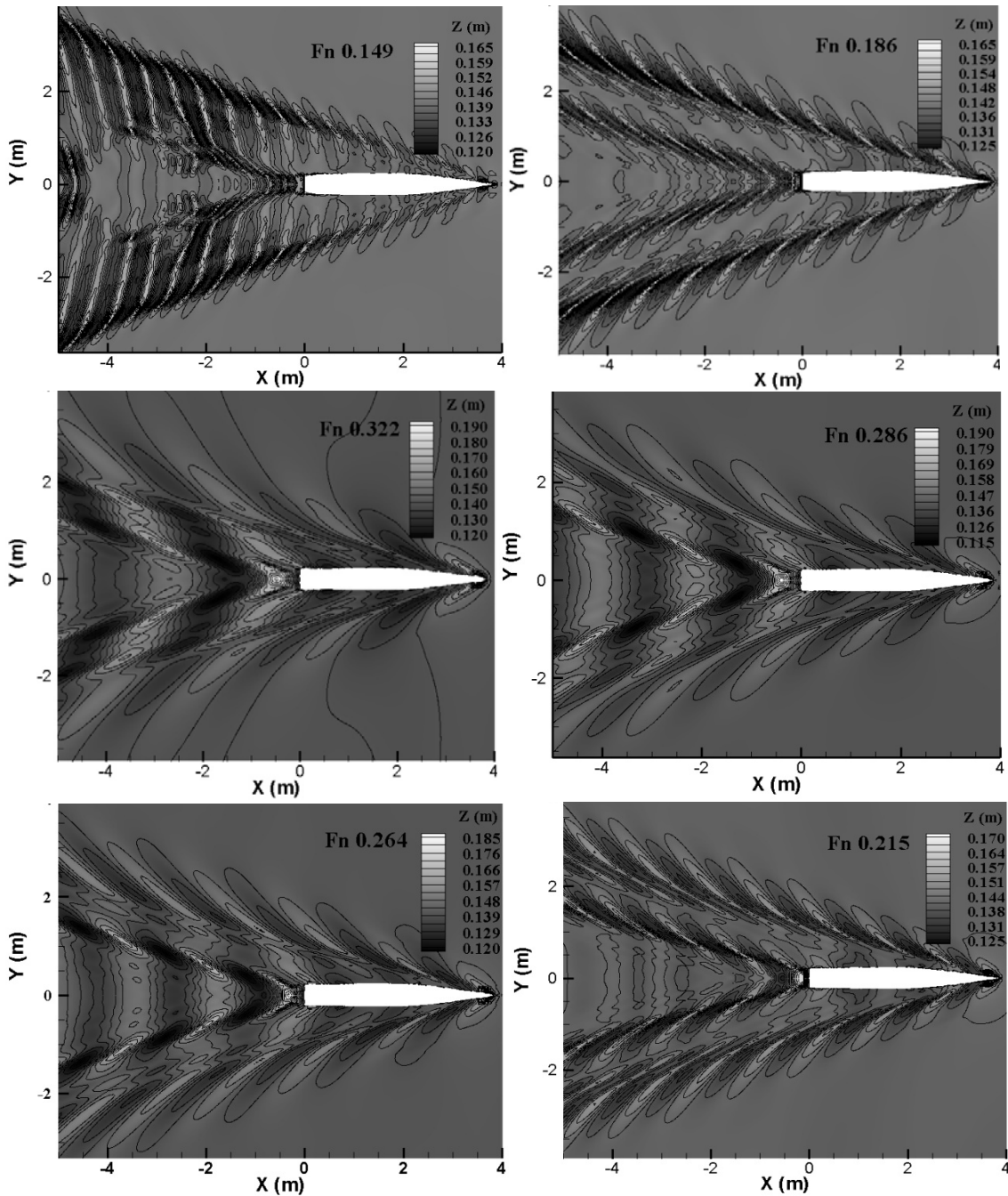


Fig. 13 Computed free surface visualization for 6 different speeds, using medium grids

Fig. 14 provides a close-up perspective view of the computed bow wave patterns and a photograph around the ship model at $Fn=0.215$. The computation shows the formation of a thin sheet of water close to the bow. Two scars are also observed in the photograph during experiment. Also in agreement with the data, the computed prediction shows a slightly more steep shoulder wave, which is different from the classical Kelvin wave patterns. Fig. 15 depicted a close-up perspective view of the computed aft wave form development and a photograph during experiment behind the model at $Fn=0.215$. Transom separation can be seen clearly both in CFD solution and the experiment.

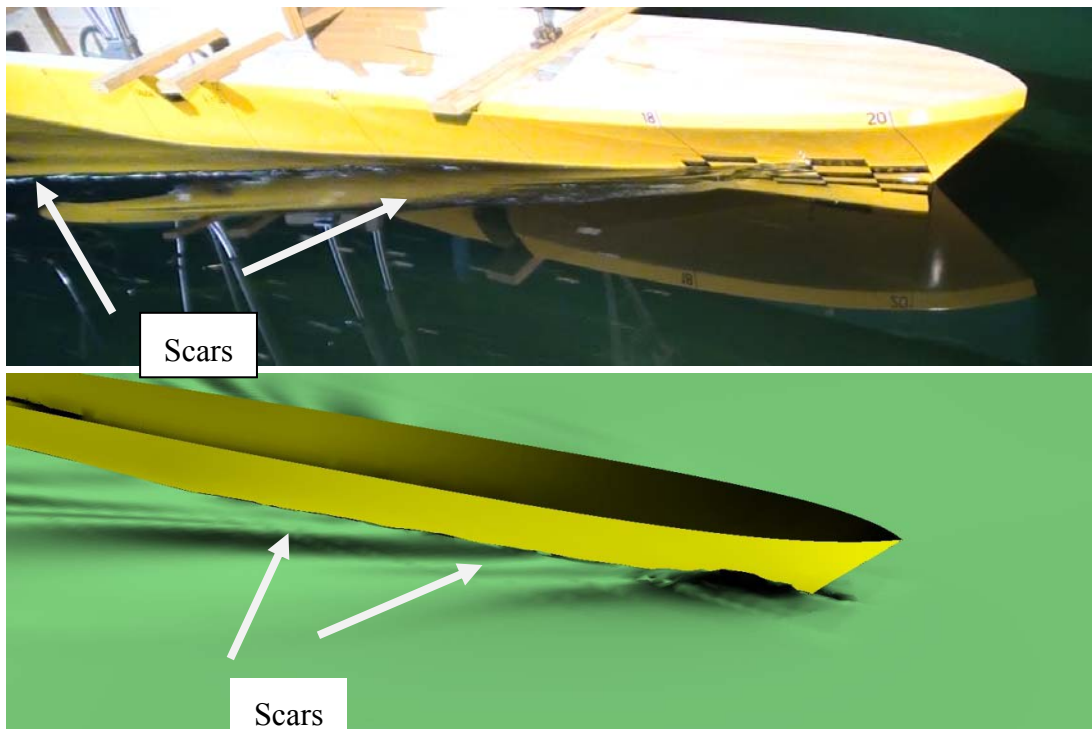


Fig. 14 Bow wave details for CFD solution (bottom) and experimental photograph (top), $Fn=0.215$

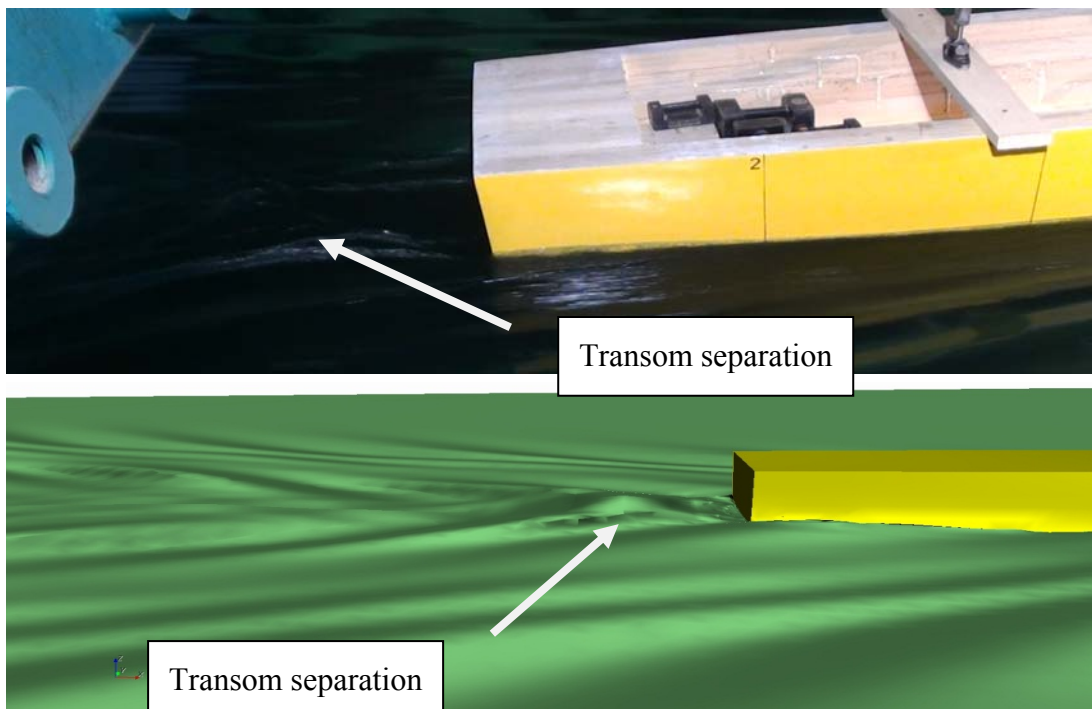


Fig. 15 Wake created behind the model, CFD solution (bottom) and experimental photograph (top), $Fn=0.215$

6. Conclusions

This paper presents the simulation and experimental results of flow field around a fast ship. Although some experimental data have been showed for validation of CFD results the main objective of this study is to assess the performance of the commercial software Star CCM+ for design, analysis and feasibility of such a simulation for shipping industry. From the simulations of the M367 ship model the following conclusions are presented:

1. Standard $k-\varepsilon$ turbulence model is in good agreement with experimental data and therefore it can be used for ship resistance investigations, except for the situations that flow separations occur.
2. For relatively higher speeds ($Fn > 0.25$) a low Reynolds number turbulence model can be more suitable to predict the resistance, but the computations will be very expensive in terms of computational time.
3. As expected the finer are the grids, the better is the accuracy at a cost of longer computation time. Reducing the grid size provides better representation of the bow and aft of the ship model. However, it also increases the computation time drastically, and sometimes the CPU may not be able to compute the huge amount of data because of memory deficiency. Several grid refinement studies were performed, and the optimum grid size were chosen for resistance calculations.
4. The experiments and computations were done for 11 different speeds from $Fn=0.103$ to $Fn=0.322$. The results show that, the ability of Star CCM+ for predicting free surface flow around model ship hull is generally satisfactory. Therefore it is suggested that Star CCM+ may be considered as a useful tool for predicting free surface flows and ship resistance for $Fn < 0.25$.
5. The form factor $(1+k)$ with the use of the standard $k-\varepsilon$ turbulence model may be easily predicted.
6. Much smaller normalized residual of the free surface elevation can be chosen in the VOF module running on a better computer.
7. For very slow flow speeds, where the wave making resistance can be negligible, double body flow approach can be used.
8. Overall results show that for medium Froude numbers $Fn < 0.25$, the computations give efficient and accurate tool to predict curves of resistance for ship flows, including time savings on case setup and CPU hours.
9. The findings are limited to the unappended model ship. For the future work, ship models with appendages are required to investigate the performance and reliability of Star CCM+ code.

Acknowledgement

The research was partly supported by Yildiz Technical University Scientific Grants Program, grant number 2011-10-01-KAP01 for which it is greatly acknowledged. The authors also thank the staff of Ata Nutku Ship Model Testing Laboratory of Istanbul Technical University for their help during the experiments.

REFERENCES

- [1] Y. Sato, H. Miyata, T. Sato: *CFD simulation of 3-dimensional motion of a ship in waves application to an advanced ship in regular heading waves*. Journal of Marine Science and Technology **4**, no. 9, 108-116 (1999).
- [2] J.J. Gorski: *Present state of numerical ship hydrodynamics and validation experiments*. Journal Offshore Mechanics and Arctic Engineering–Trans. ASME **124**, no. 2, 74-80 (2002).
- [3] U.T. Bulgarelli, C. Lugbi, M. Landrini: *Numerical modeling of free-surface flows in ship hydrodynamics*. International Journal for Numerical Methods in Fluids **43**, no. 3, 465- 481 (2003).
- [4] N. Parolini, A. Quarteroni: *Mathematical Models and Numerical Simulations for the America's Cup*, Comp. Meth. Appl. Mech. Eng **194**, no. 9-11, 1001-1026 (2005).
- [5] Y. Ahmed, C. Guedes Soares: *Simulation of free surface flow around a VLCC hull using viscous and potential flow methods*. Ocean Engineering **36**, no. 9, 691-696 (2009).
- [6] D. Sridhar, T.V.K. Bhanuprakash, H.N. Das: *Frictional resistance calculations on a ship using CFD*. International Journal of Computer Applications **11**, no. 5, 24-31, (2010).
- [7] J. Wackers, B. Koren, H.C. Raven, A. van der Ploeg, A.R. Starke, G.B. Deng, P. Queutey, M. Visonneau: *Free-surface viscous flow solution methods for ship hydrodynamics*. Arch Comput Methods Eng **18**, 1–41, (2011).
- [8] T. Xing, S. Bhushan, F. Stern: *Vortical and turbulent structures for KVLCC2 at drift angle 0, 12, and 30 degrees*. Ocean Engineering **55**, 23–43, (2012).
- [9] T.Q. Li, J. Matusiak, R. Lehtimati: *Numerical simulation of viscous flows with free surface around realistic hull forms with transom*. International Journal for Numerical Methods in Fluids **37**, no. 5, 601-624, (2001).
- [10] A. Leroyer, J. Wackers, P. Queutey, E. Guilmineau: *Numerical strategies to speed up CFD computations with free surface - Application to the dynamic equilibrium of hulls*. Ocean Engineering **38**, no. 17-18, 2070-2076, (2011).
- [11] B.J. Guo, S. Steen, G.B. Deng: *Seakeeping prediction of KVLCC2 in head waves with RANS*. Applied Ocean Research **35**. 56-57, (2012).
- [12] M. Kandasamy, S.K. Ooi, P. Carrica, F. Stern, E.F. Campana, D. Peri, P. Osborne, J. Cote, N. Macdonald, N. De Wall: *CFD validation studies for a high-speed foil-assisted semi-planning catamaran*. Journal of Marine Science and Technology **16**, no 2, 157-167, (2011).
- [13] T. Takai, M. Kandasamy, F. Stern: *Verification and validation study of URANS simulations for an axial waterjet propelled large high-speed ship*. Journal of Marine Science and Technology **16**, no. 4, 434-447, (2011).
- [14] K.C. Seo, M. Atlar, R. Sampson: *Hydrodynamic development of inclined keel hull-resistance*. Ocean Engineering **47**, 7–18, (2012).
- [15] S.V. Patankar, D.B. Spalding: *A calculation procedure for heat, mass and momentum transfer in three-dimensional parabolic flows*. Int. J. Heat Mass Transfer **15**, no. 10, 1787-1806, (2005).
- [16] S.A. Dixit, O.N. Ramesh: *Determination of skin friction in strong pressure-gradient equilibrium and near equilibrium turbulent boundary layers*. Experiment Fluids **47**, no. 6, 1045-1058, (2009).
- [17] B. Sener: *Developing of frigate type hull form serie and hydrodynamic form optimization*. Ph.D. Thesis, Yıldız Technical University, Istanbul, Turkey, 2012.
- [18] K.S. Min, S.H. Kang: *Study on the form factor and full-scale ship resistance prediction method*. Journal of Marine Science and Technology **15**, no. 2, 108-118, (2010).
- [19] C.W. Prohaska: *A simple method for the evaluation of the form factor and low speed wave resistance*. Proceedings of the 11th ITTC, 65, 1966.
- [20] O. Goren, D.B. Danisman: *Uncertainty analysis of resistance tests for 85.32 m 1/40 scale asphalt tanker model*. Ata Nutku Ship model Testing Laboratory, Report no:01.01/1, 2010.

Submitted: 01.03.2013

Accepted: 18.11.2013.

Yavuz Hakan Ozdemir
Faculty of Naval Arch. and Maritime, Yildiz Tech.
Univ, Istanbul, Turkey.
Baris Barlas (e-mail: barlas@itu.edu.tr)
Faculty of Naval Arch. and Ocean Engin., Istanbul
Tech. Univ., Istanbul, Turkey.
Tamer Yilmaz
Seyfettin Bayraktar
Faculty of Naval Arch. and Maritime, Yildiz Tech.
Univ., Istanbul, Turkey.